Determination of Proton Radii of Neutron-rich Oxygen Isotopes

Satbir Kaur

DALHOUSIE UNIVERSITY

SAINT MARY'S UNIVERSITY SINCE 1802

Outline

- Introduction
  - Nuclear landscape and neutron-rich nuclei.
- Scientific Motivation
  - Motivation to study oxygen isotopes.
  - Importance of Proton Radii (R_p)
- Methods to measure R_p and Charge changing cross sections (σ_{cc})
- Experimental Setup
- Results
- Summary

Neutron-rich nuclei

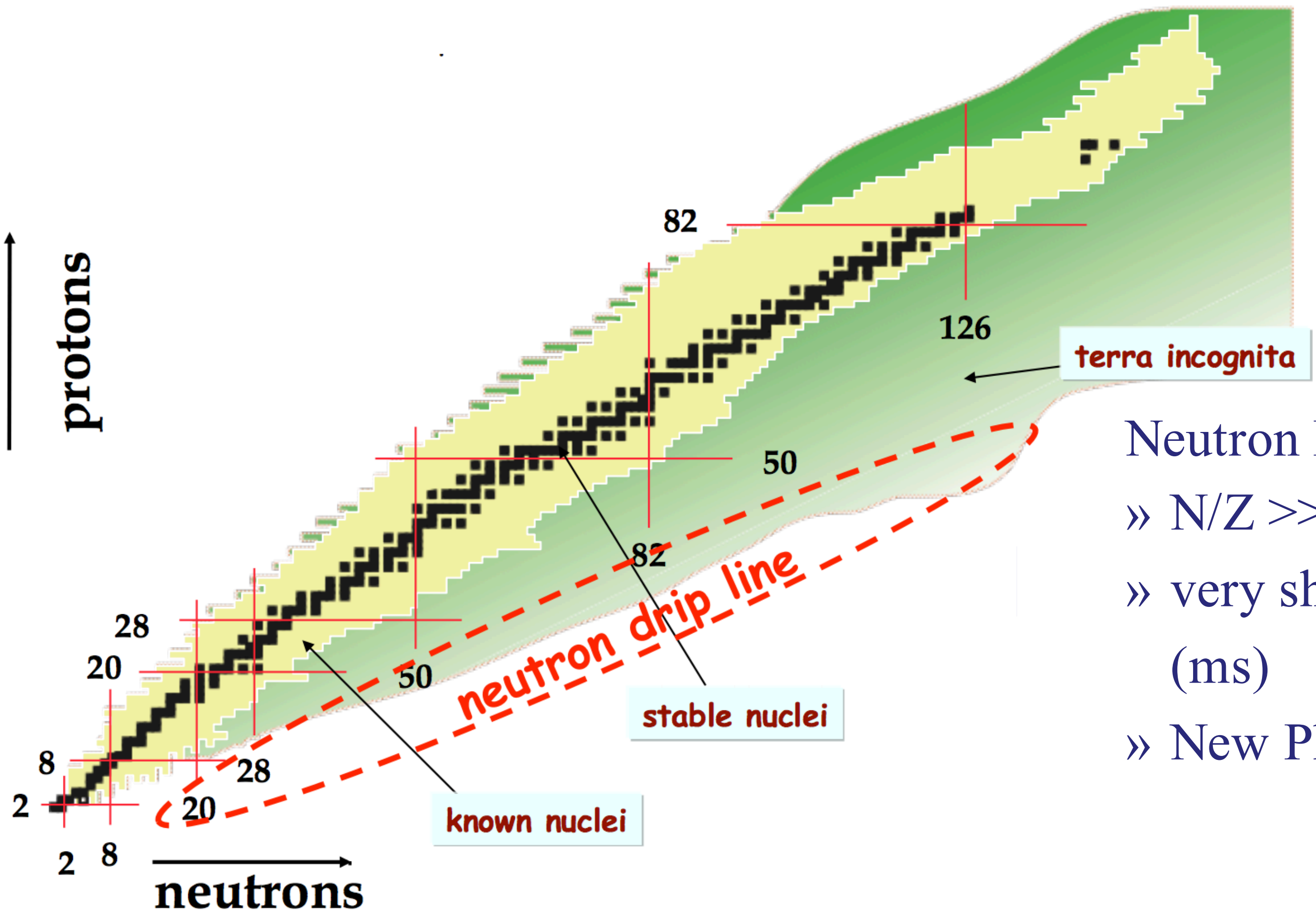

Neutron Rich Nuclei

» N/Z >>1

» very short half life (ms)

» New Physics.

Outline

- Introduction
  - Nuclear landscape and neutron-rich nuclei.
- Scientific Motivation
  - Motivation to study oxygen isotopes.
  - Importance of Proton Radii
- Methods to measure Rp and Charge changing cross sections (σcc)
- Description of Experimental Setup
- Results
- Summary

Interesting neutron-rich oxygen isotopes.

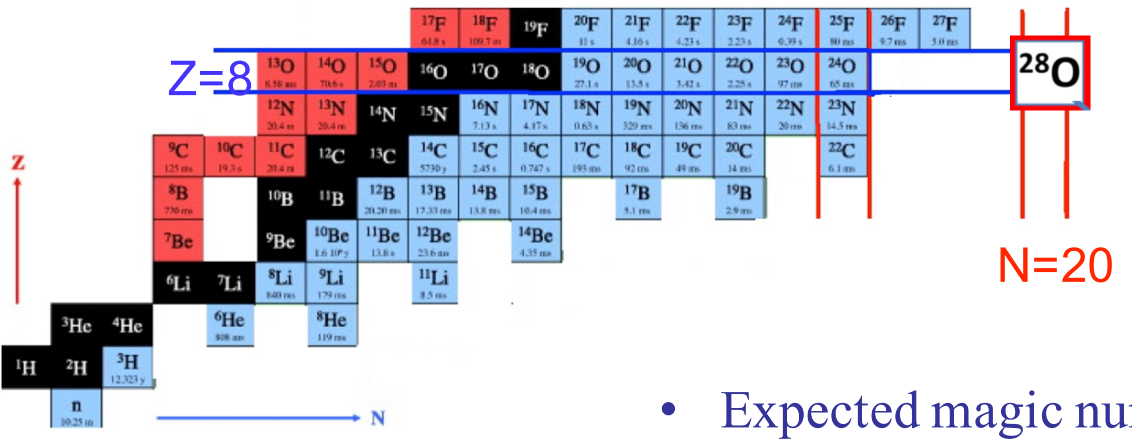

- Expected magic number nucleus

Interesting neutron-rich oxygen isotopes.

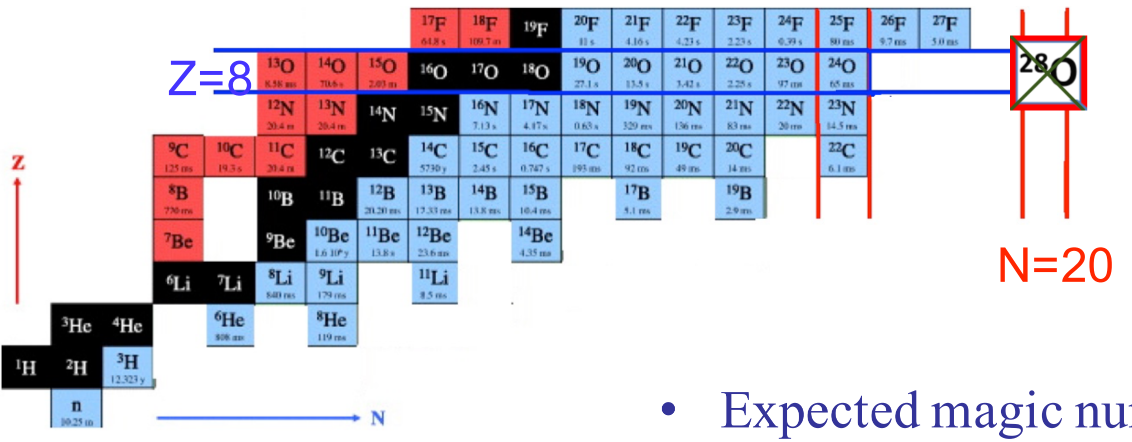

- Expected magic number nucleus ^{28}O unbound
  (Tarasov et al., 1997)

Interesting neutron-rich oxygen isotopes.

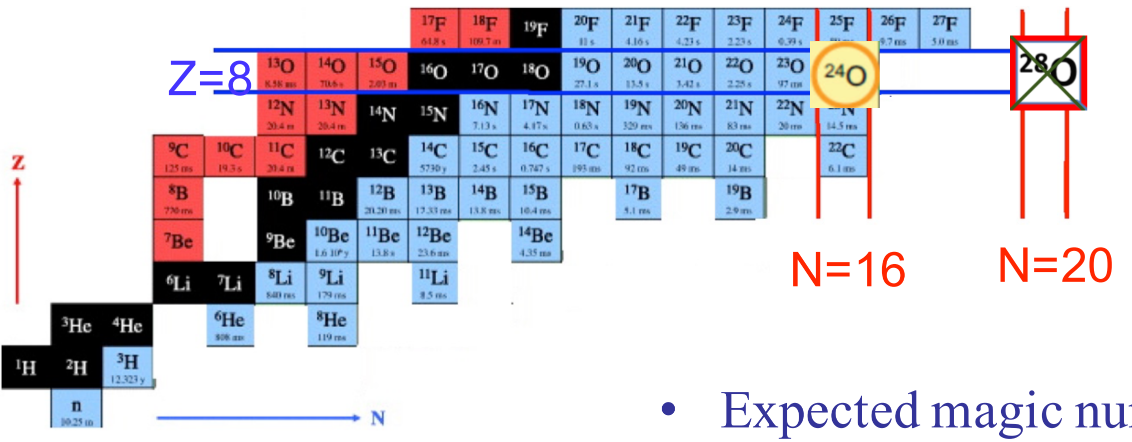

- Expected magic number nucleus ^{28}O unbound
  (Tarasov et al., 1997)
- Neutron drip line of O at ^{24}O (N=16).
  (Hoffman et al 2008, Lunderberg et al 2012).

Interesting neutron-rich oxygen isotopes.

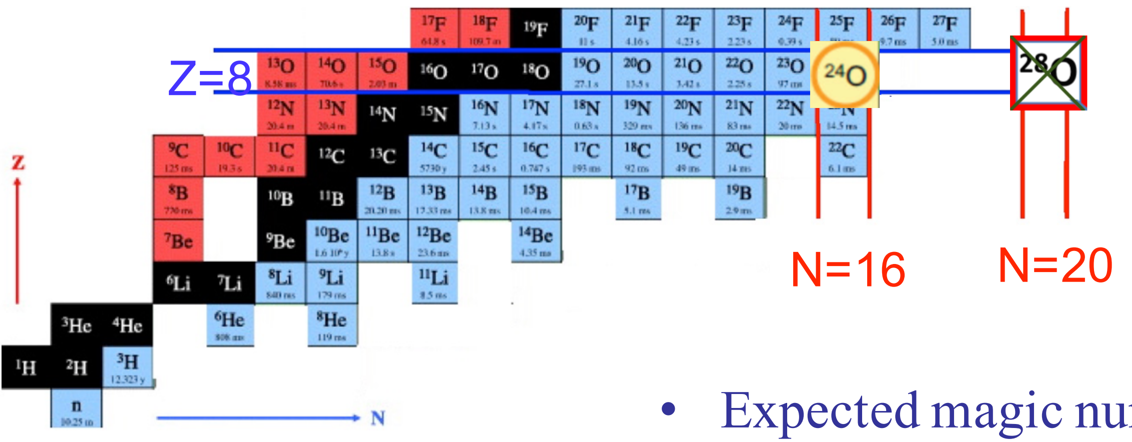

- Expected magic number nucleus ^{28}O unbound
  (Tarasov et al., 1997)

- Neutron drip line of O at ^{24}O.
  (Hoffman et al 2008, Lunderberg et al 2012).

- ^{24}O doubly magic with new magic number (N =16).
  (A. Ozawa et al., (2000), R. Kanungo et al., (2002).) R. Kanungo,(2009))

Interesting neutron-rich oxygen isotopes.

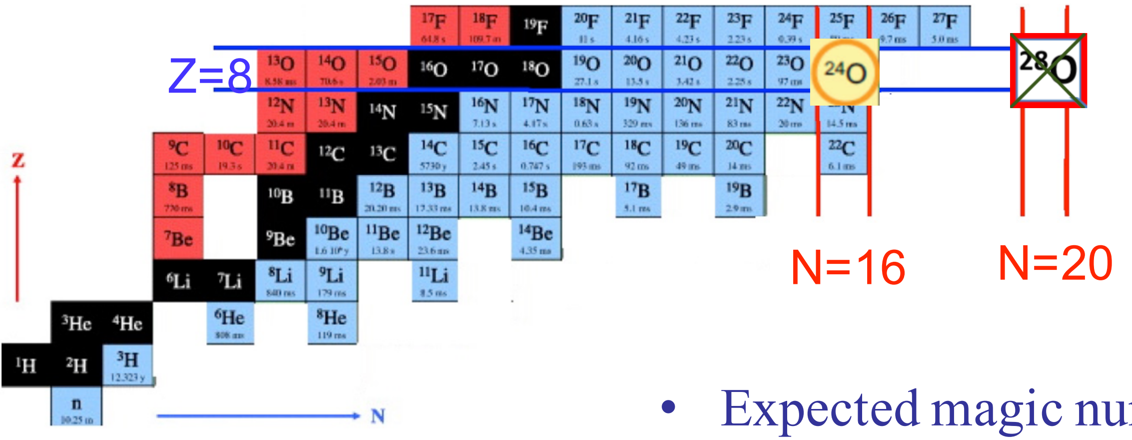

- Expected magic number nucleus ^{28}O unbound
  (Tarasov et al., 1997)

- Neutron drip line of O at ^{24}O.
  (Hoffman et al 2008, Lunderberg et al 2012).

- ^{24}O doubly magic with new magic number (N =16).
  (A. Ozawa et al., (2000), R. Kanungo et al., (2002).) R. Kanungo,(2009))

- To yield the drip line at ^{24}O, 3NF required .

Interesting neutron-rich oxygen isotopes.

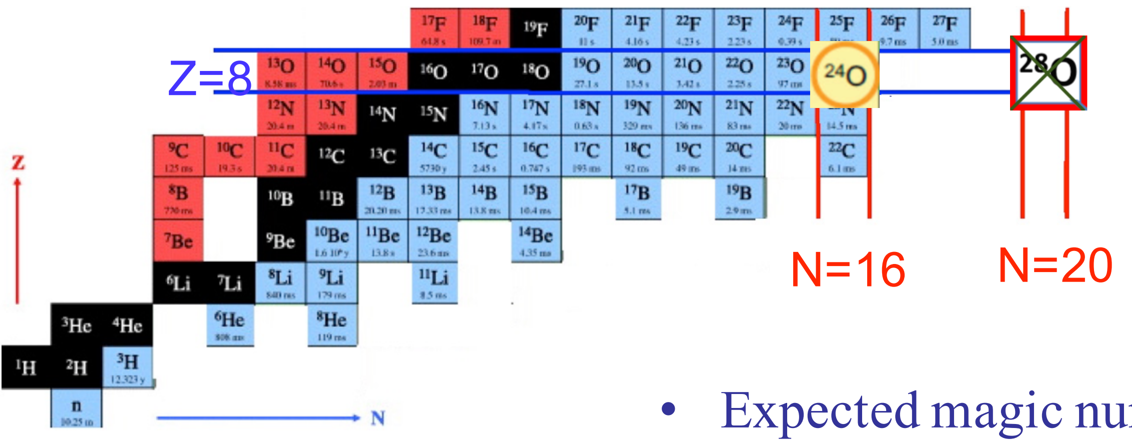

- Expected magic number nucleus ^{28}O unbound
  (Tarasov et al., 1997)

- Neutron drip line of O at ^{24}O.
  (Hoffman et al 2008, Lunderberg et al 2012).

- ^{24}O doubly magic with new magic number (N =16).
  (A. Ozawa et al., (2000), R. Kanungo et al., (2002).) R. Kanungo,(2009))

- To yield the drip line at ^{24}O, 3NF required .

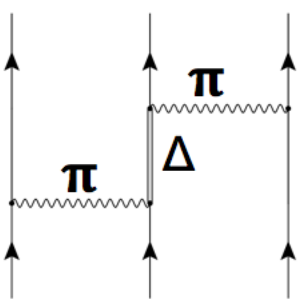

An example of 3N force

Interesting neutron-rich oxygen isotopes.

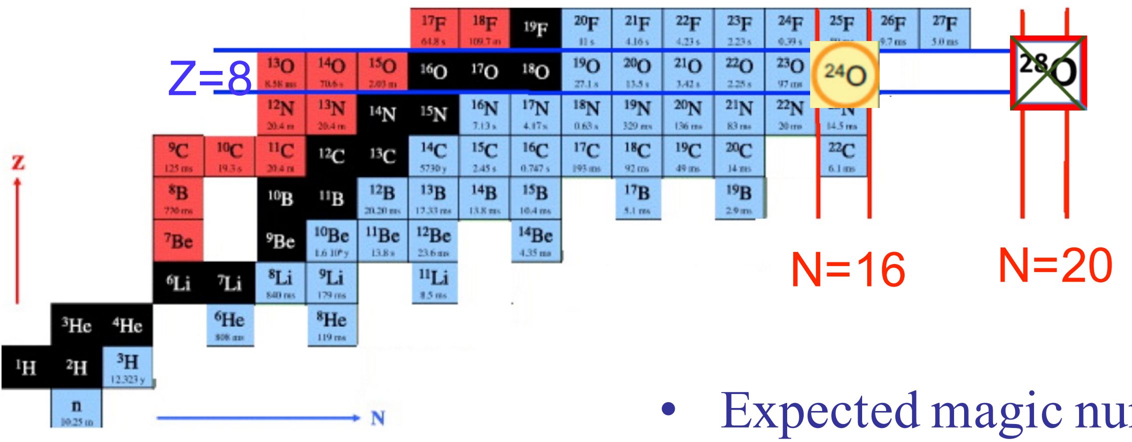

Ground state energies with 3NF show a kink at N= 16.

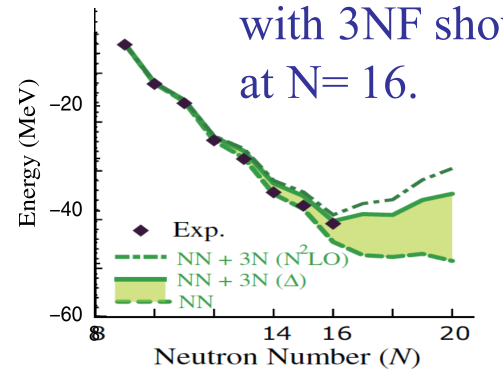

Otsuka et al., (2010)

- Expected magic number nucleus ^{28}O unbound
  (Tarasov et al., 1997)
- Neutron drip line of O at ^{24}O.
  (Hoffman et al 2008, Lunderberg et al 2012).
- ^{24}O doubly magic with new magic number (N =16).
  (A. Ozawa et al., (2000), R. Kanungo et al., (2002).) R. Kanungo,(2009))
- To yield the drip line at ^{24}O, 3NF required .

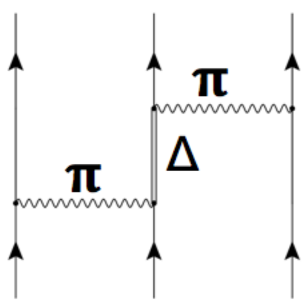

An example of 3N force

Outline

- Introduction
  - Nuclear landscape and neutron-rich nuclei.
- Scientific Motivation
  - Motivation to study oxygen isotopes.
  - Importance of Proton Radii
- Methods to measure Rp and Charge changing cross sections (σcc)
- Description of Experimental Setup
- Results
- Summary

Test of ab-intio theories

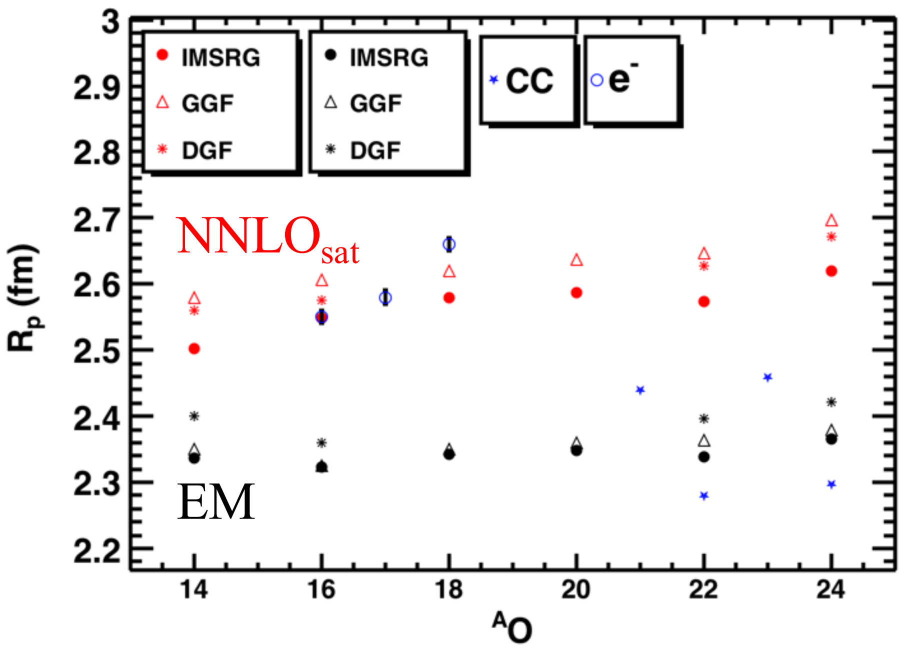

Calculated R_p with EM and $NNLO_{sat}$ interaction

IMSRG, SCGF calculations (Lapoux et al., (2016)), Couple cluster (CC) (Hagen et. al, (2012)

Rp e^- scattering experiment (Atomic Data and Nuclear Data Tables, 2013)

Proton radii of neutron rich oxygen isotopes not measured till date.

Determination of neutron skin

Neutron skin Thickness→ $\delta R = \langle r_n^2 \rangle^{1/2} - \langle r_p^2 \rangle^{1/2}$

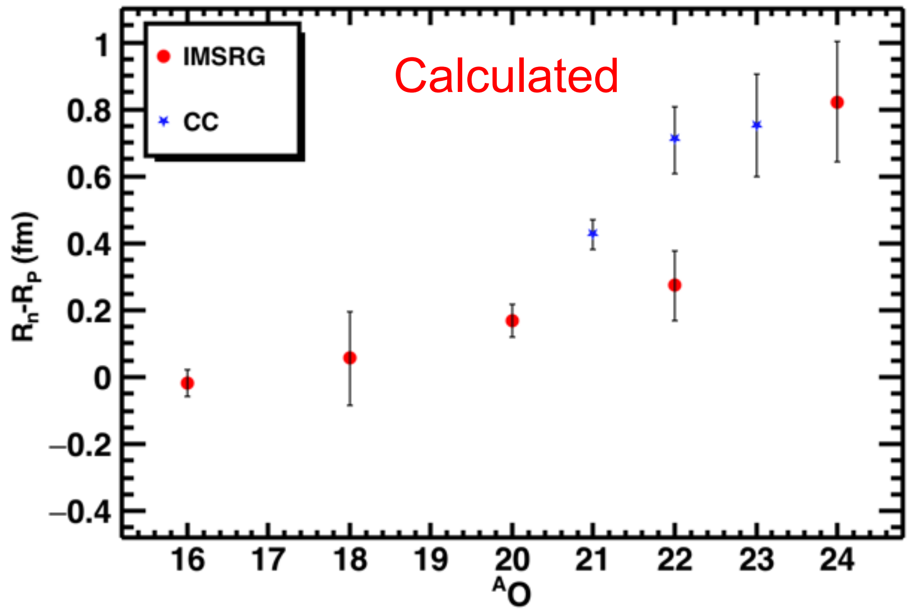

Neutron skin calculated from measured R_m and calculated R_p.

Rn determined using matter radii (R_m) from A. Ozawa et al., (2001)

R_p data required to determine neutron skin thickness.

Outline

- Introduction
  - Nuclear landscape and neutron-rich nuclei.
- Scientific Motivation
  - Motivation to study oxygen isotopes.
  - Importance of Proton Radii
- Methods to measure R_p and Charge changing cross sections (σ_{cc})
- Description of Experimental Setup
- Results
- Summary

Techniques to measure Charge radii

Electron Scattering :

$$F(q) = \frac{4\pi}{qZ} \int_0^\infty \rho_{ch}(r) \sin(qr) r \, dr$$

Limited to long lived nuclei only

F(q) carries information about charge distributions.

Isotope shift: change in energy of atomic levels of different isotopes.

Limitations

- high intensity beams with low energy difficult to produce for very short lived nuclei.
- Not applicable to all neutron rich nuclei.

Proton radii from Charge Changing Cross Sections (σ_{cc})

It is the cross-section for reactions leading to any change of the atomic number of the projectile nucleus.

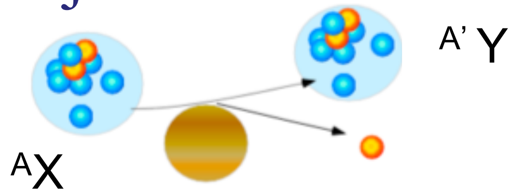

Principle of Measurement : Transmission type measurement

Incident beam (I_0)

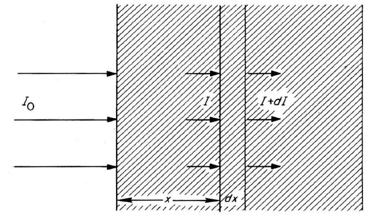

Unreacted beam

$$I = I_0 e^{-\sigma_R t}$$

$$N_{sameZ} = N_0 e^{-\sigma_{cc} t}$$

$$\sigma_{cc} = \frac{1}{t} ln \frac{N_o}{N_{sameZ}}$$

Proton radii from Charge Changing Cross Sections (σ_{cc})

It is the cross-section for reactions leading to any change of the atomic number of the projectile nucleus.

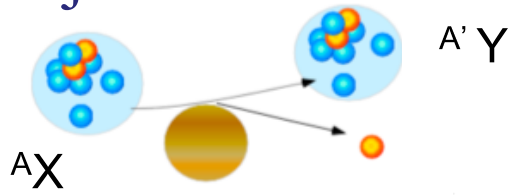

Principle of Measurement : Transmission type measurement

Incident beam (I_0)

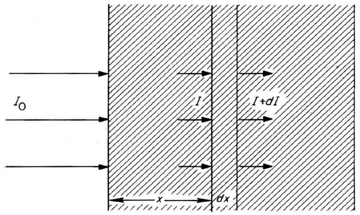

Unreacted beam

$$I = I_0 e^{-\sigma_R n d}$$

$$\sigma_{cc} = \frac{1}{t} ln \frac{\left(\frac{N_{sameZ}}{N_{in}}\right)_{R_{out}}}{\left(\frac{N_{sameZ}}{N_{in}}\right)_{R_{in}}}$$

Target out

Target in

Outline

- Introduction
  - Nuclear landscape and neutron-rich nuclei.
- Scientific Motivation
  - Motivation to study oxygen isotopes.
  - Importance of Proton Radii
- Methods to measure R_p and Charge changing cross sections (σ_{cc})
- Description of Experimental Setup
- Results
- Summary

Detector Setup

$^{16-24}$O produced from fragmentation of 1*A* GeV ^{40}Ar beam at Fragment Separator ,GSI, Germany.

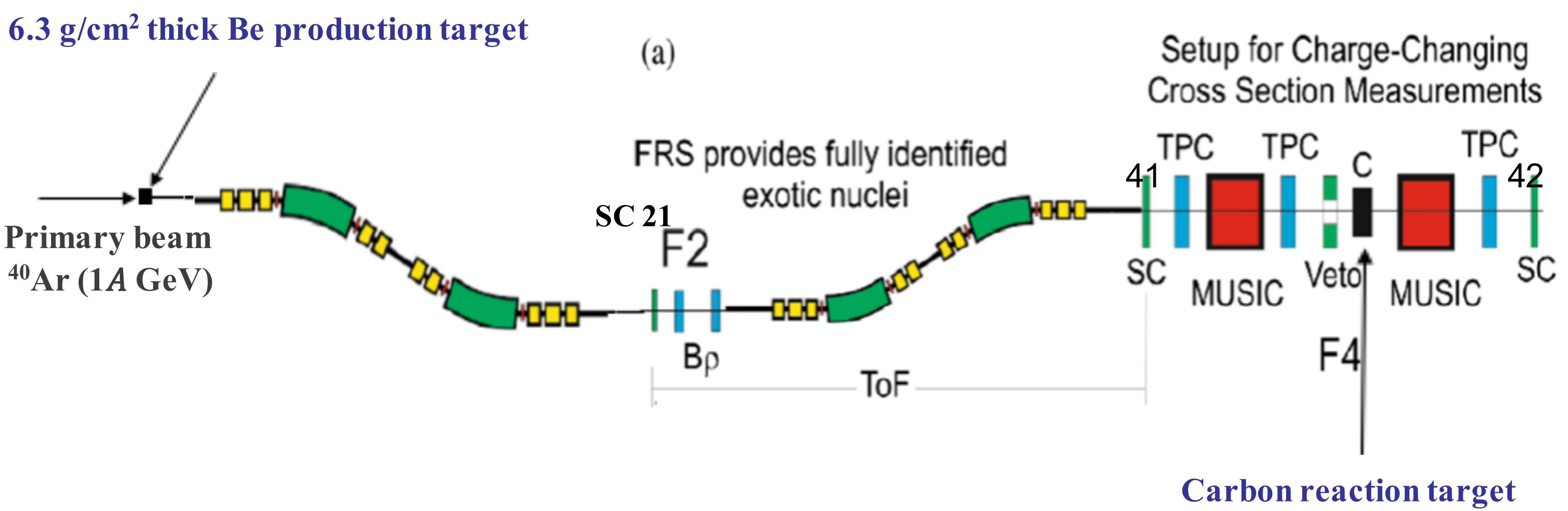

Particle Identification Spectrum

$$\frac{A}{Z} = \frac{e}{u}\frac{B\rho}{\gamma\beta c}$$

Magnetic rigidity, $B\rho = B\rho_{central}\left(1 - \frac{M_B x_{F2} - x_{F4}}{D_B}\right)$

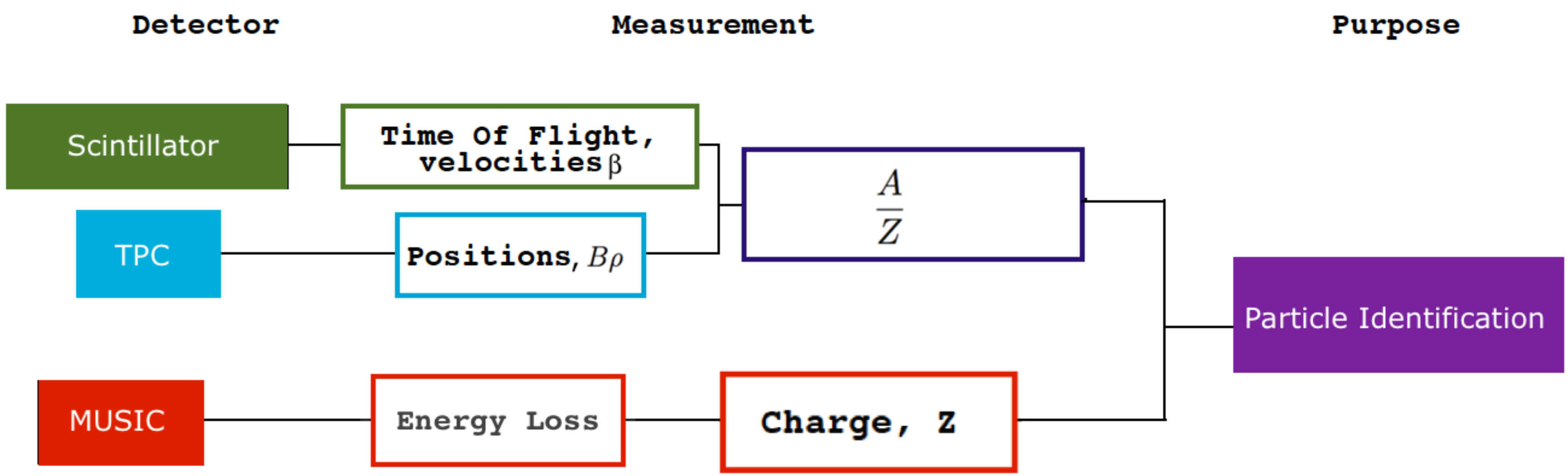

Multisampling Ionization Chamber

Particle Identification Spectrum

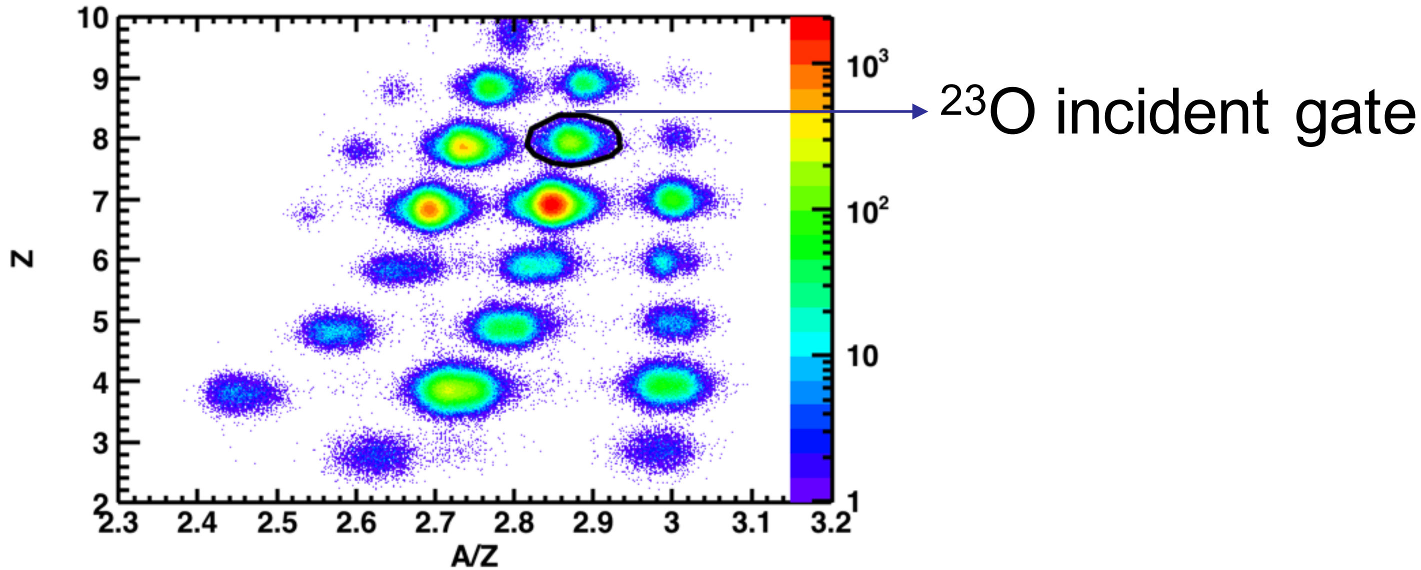

PID after removing spurious events

PID spectrum for ^{23}O before the target

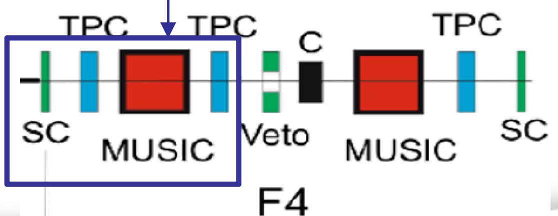

Z identification after the target

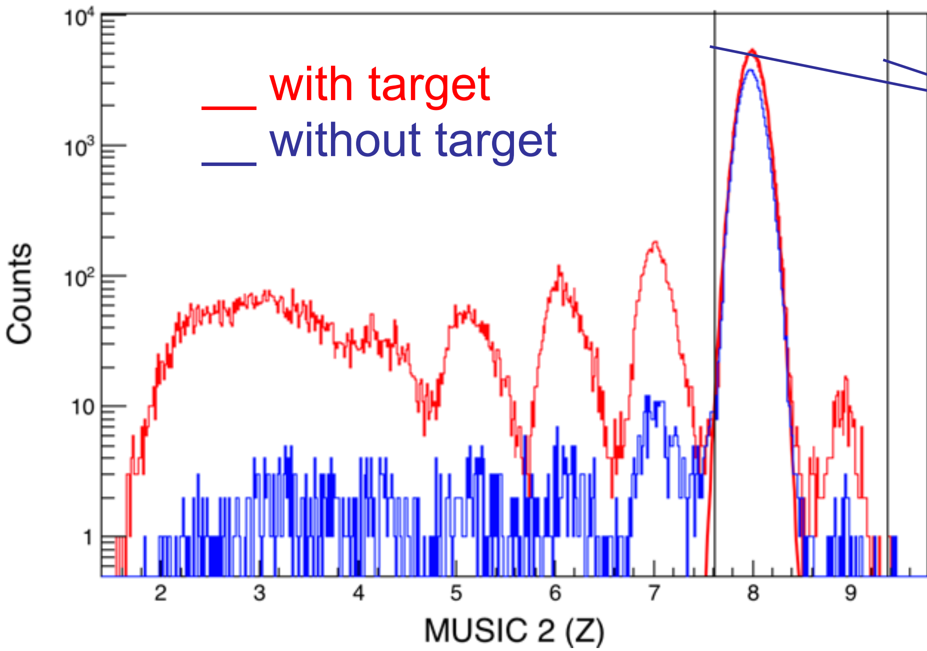

N_{sameZ} gate for ^{23}O

3.5 σ of Z=8 and Z=9 Peak

Transmission ratio $(R) = \frac{N_{sameZ}}{N_{in}}$

$$\sigma_{cc} = \frac{1}{t} ln \frac{R_{out}}{R_{in}}$$

Energy loss spectrum in MUSIC detector after the target with ^{23}O incident beam selected.

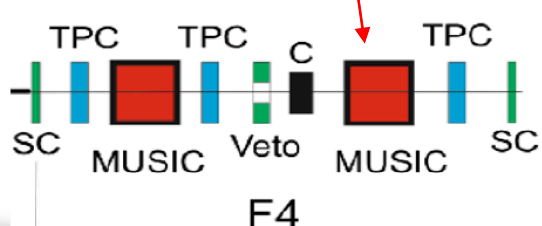

Outline

- Introduction
  - Nuclear landscape and neutron-rich nuclei.
- Scientific Motivation
  - Motivation to study oxygen isotopes.
  - Importance of Proton Radii
- Methods to measure R_p and Charge changing cross sections (σ_{cc})
- Description of Experimental Setup
- Results
- Summary

Results

σ_{cc} of O isotopes

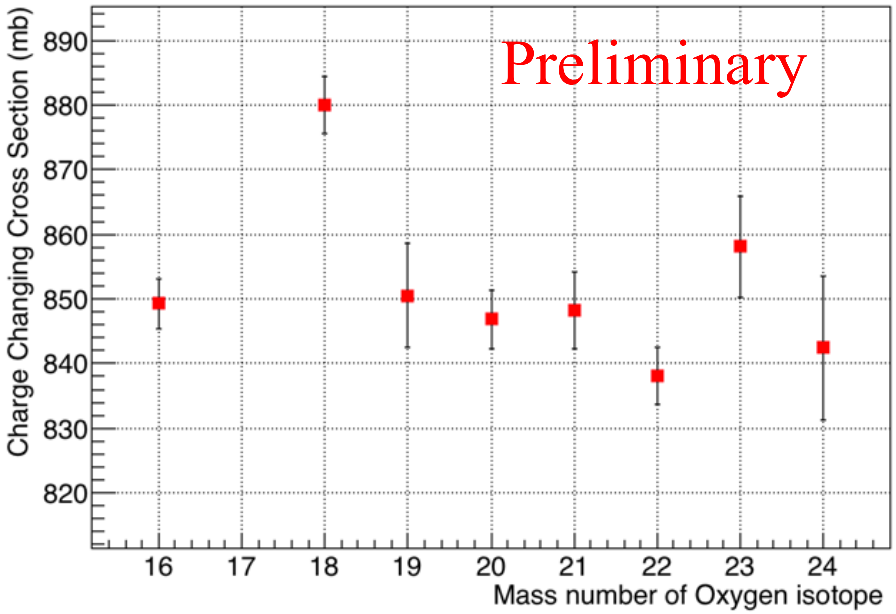

- An increase in σ_{cc} of ^{18}O.
- The σ_{cc} of $^{19\text{-}21}$O shows flat trend.
- The σ_{cc} of ^{22}O decreases followed by an increase for ^{23}O.

R_p of ^{16}O and ^{18}O from the σ_{cc}

Glauber Model formalism

$$\sigma_{\rm cc} = \int d\boldsymbol{b}\, P_{\rm cc}(\boldsymbol{b}).$$

$$P_{\rm cc}^{\rm dir}(\boldsymbol{b}) = 1 - \exp\left(-2 \sum_{N=p,n} \iint d\boldsymbol{s}\, d\boldsymbol{t}\, T_{Proj}^{(p)}(\boldsymbol{s}) T_{Target}^{(N)}(\boldsymbol{t}) \times {\rm Re}\,\Gamma_{pN}(\boldsymbol{b} + \boldsymbol{s} - \boldsymbol{t})\right),$$

where $T_{Proj}^{(p)}(\boldsymbol{s}) = \int_{-\infty}^{\infty} dz\, \rho_P^{(p)}(\boldsymbol{r})$ → Proton density

and $\Gamma_{NN}(\boldsymbol{b}) = \frac{1 - i\alpha}{4\pi\beta}\sigma_{NN}^{\rm tot}\exp\left(-\frac{\boldsymbol{b}^2}{2\beta}\right)$

(NN cross section) (finite range parameter)

R_p of ^{16}O and ^{18}O from the σ_{cc}

Glauber Model formalism

$$\sigma_{cc} = \int d\boldsymbol{b}\, P_{cc}(\boldsymbol{b}).$$

$$P_{cc}^{dir}(\boldsymbol{b}) = 1 - \exp\left(-2\sum_{N=p,n}\iint d\boldsymbol{s}\, d\boldsymbol{t}\, T_{Proj}^{(p)}(\boldsymbol{s}) T_{Target}^{(N)}(\boldsymbol{t}) \times \mathrm{Re}\,\Gamma_{pN}(\boldsymbol{b}+\boldsymbol{s}-\boldsymbol{t})\right),$$

where $T_P^{(p)}(\boldsymbol{s}) = \int_{-\infty}^{\infty} dz\, \rho_P^{(p)}(\boldsymbol{r})$ → Proton density

and $\Gamma_{NN}(\boldsymbol{b}) = \frac{1-i\alpha}{4\pi\beta}\sigma_{NN}^{tot}\exp\left(-\frac{\boldsymbol{b}^2}{2\beta}\right)$

(NN cross section) (finite range parameter)

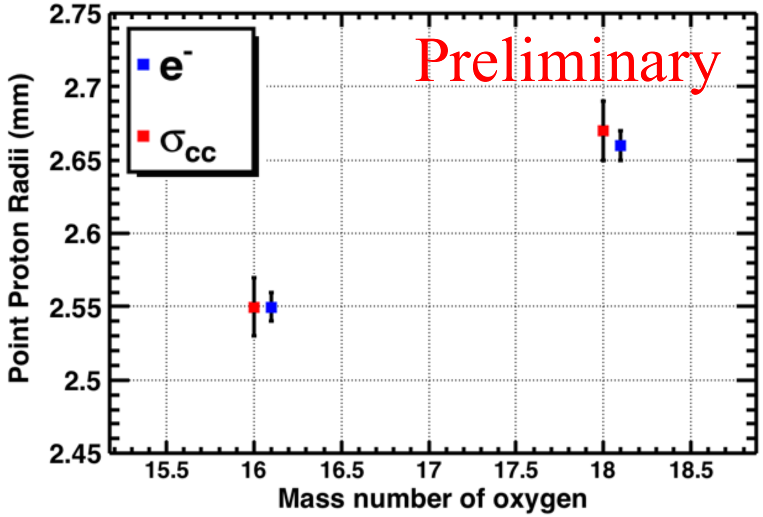

R_p for ^{16}O and ^{18}O Agree with e^- scattering experiments.

Summary

» σ_{cc} measurement is a new method to determine R_p of neutron-rich isotopes.

» R_p determined from σ_{cc} for ^{16}O and ^{18}O are consistent with electron scattering experiment.

» The first measurement of R_p for $^{19-24}O$ is underway.

» The measured Rp will be used for first determination of neutron skin of O isotopes.

» The measured Rp will also verify various newly developed models.

Acknowledgements

Supervisor : Dr. Rituparna Kanungo

W.Horiuchi, F. Ameil, J. Atkinson, Y. Ayyad, S. Bagchi, D. Cortina-Gil, I. Dillmann, A. Estrade, A. Evdokimov, F. Farinon, H.Geissel, G. Guastalla, R. Janik, R. Knobel, J. Kurcewicz, Yu. A. Litvinov, M. Marta, M.Mostazo, I. Mukha, C. Nociforo, H.J. Ong, S. Pietri, A. Prochazka, C. Scheidenberger, B. Sitar, P.Strmen, M. Takechi, J. Tanaka, I. Tanihata, S.Terashima, J. Vargas, H.Weick, and J. S.Winfield

SAINT MARY'S UNIVERSITY SINCE 1802
One University. One World. Yours.

DALHOUSIE UNIVERSITY

CINP ICPN

GSI Helmholtzzentrum für Schwerionenforschung GmbH

NSERC CRSNG

Thank You

Particle Identification(PID) for ^{23}O

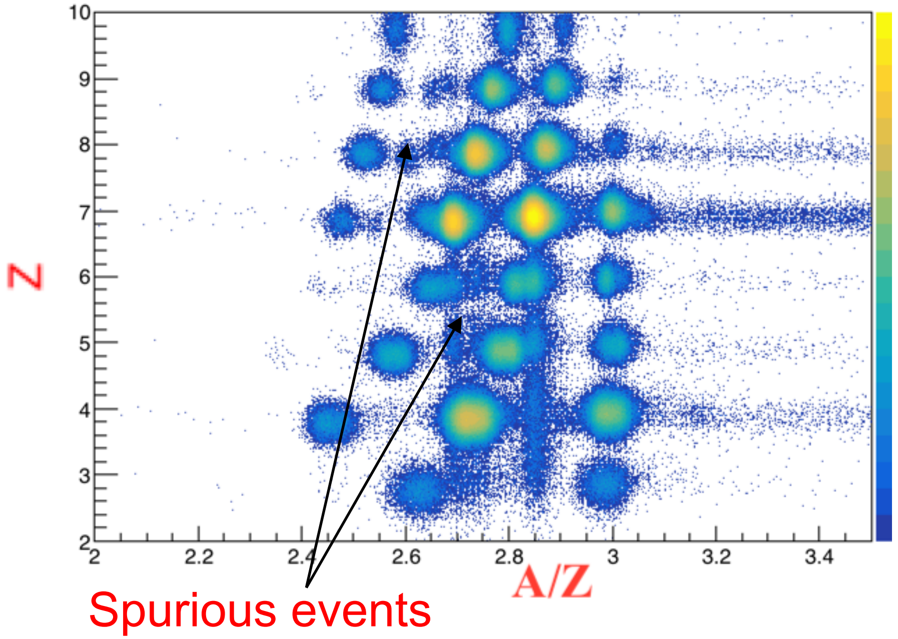

PID after veto rejection

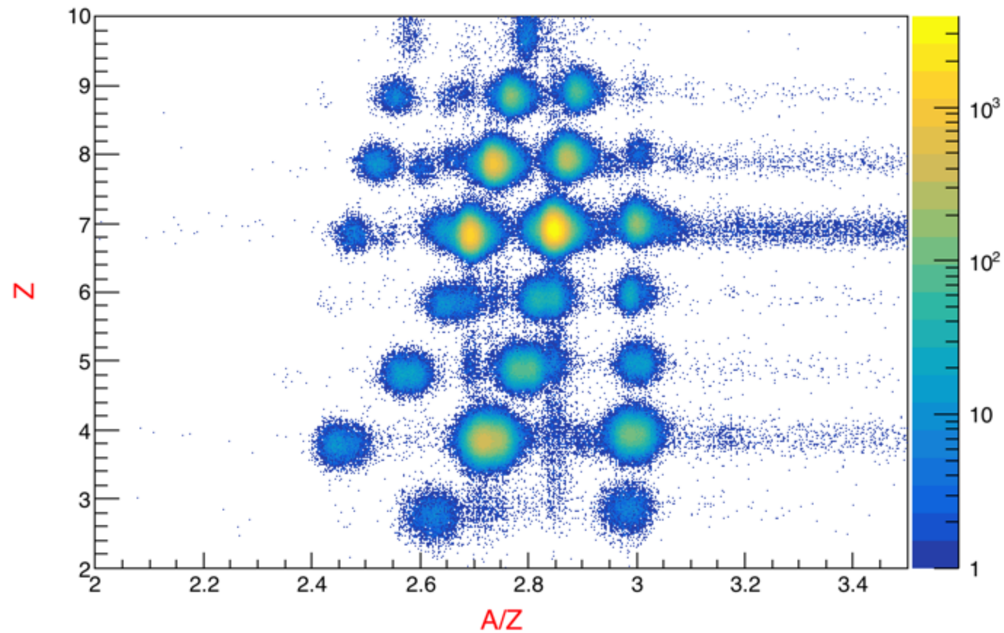

Veto Detector→ Plastic scintillator to reject particles hitting at the edge of target

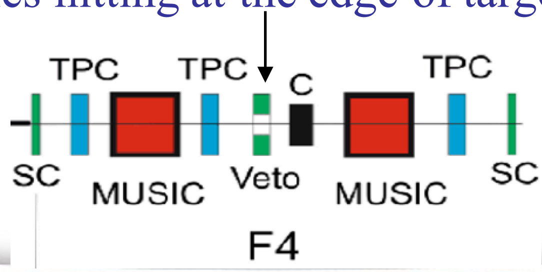

Glauber Model and σcc

Glauber Model applied successfully to Boron isotopes

$$\Gamma_{NN}(\boldsymbol{b}) = \frac{1-i\alpha}{4\pi\beta}\sigma_{NN}^{\text{tot}}\exp\left(-\frac{\boldsymbol{b}^2}{2\beta}\right)$$

where α is the ratio of the real to the imaginary part of (σ_{NN}) scattering amplitude in the forward direction,

(σ_{pn}^{tot}) is the pp (pn) total cross sections,

β is the slope parameter of the elastic scattering differential cross section.

$$\beta_{pN} = \frac{1+\alpha_{pN}^2}{16\pi}\sigma_{pN}^{\text{tot}}$$

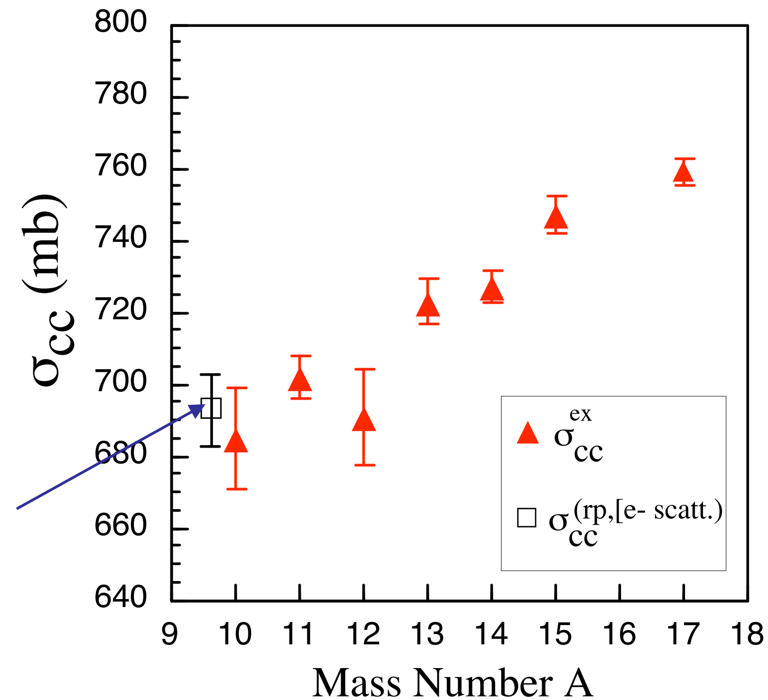

(A. Estradé et al., Phys. Rev. Let.113, 132501,(2014)

Limitations of isotope shift

Isotope shift: change in energy of atomic levels of different isotopes.

$$\delta \nu_{A,A'} = \delta \nu^{MS}_{A,A'} + K_{FS}\delta\langle r^2\rangle_{A,A'}$$

Limitations

- low energy and good intensity beams difficult to produce for all neutron rich isotopes.
- Mass shift term dominates for O.
- Many body calculations complicated

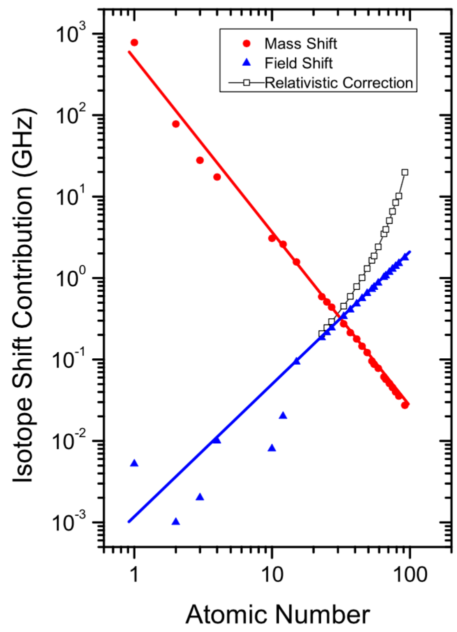

K.Blaum et al.Phys. Scr. T152 (2013) 014017

Multisampling Ionization Chamber(MUSIC)

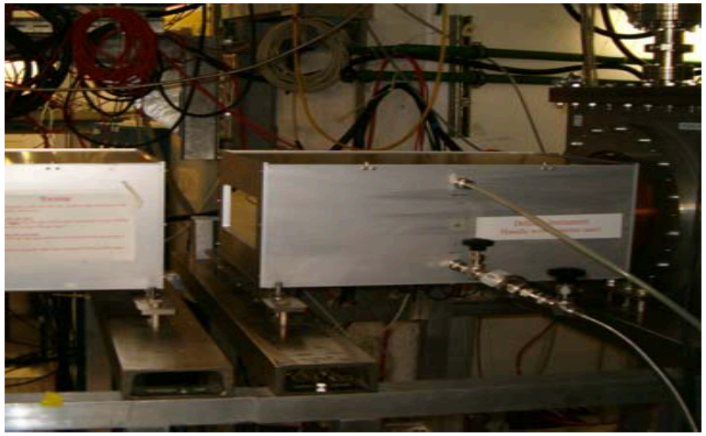

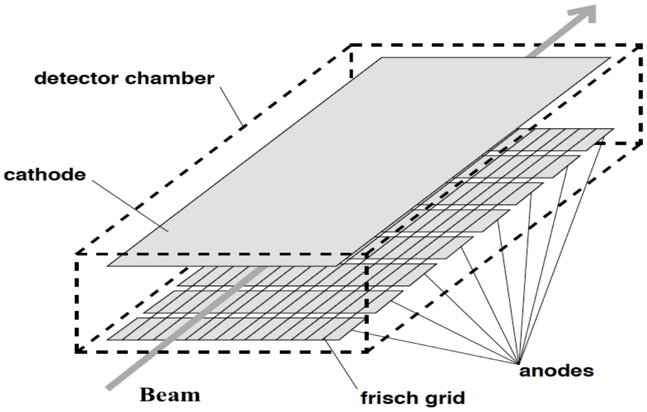

'ounting Gas -CF_4
ressure- 1 bar
'imensions-200 x 80 x
00mm

Bethe formula for energy loss

$$\frac{-dE}{ds} = \frac{4\pi Z_p^2}{m_e c^2 \beta^2} \left(\frac{e^2}{4\pi\epsilon_0} \right)^2 Z_t N_t \left(\ln \frac{2 m_e v^2}{I} - \ln(1-\beta^2) - \beta^2 \right)$$

Geometric average of signals from each anode gives us the energy loss

$$dE_{raw} = (e_1 \cdot e_2 \cdot e_3 \cdot e_4 \cdot e_5 \cdot e_6 \cdot e_7 \cdot e_8)^{1/8}$$

Calibration of MUSIC Detector

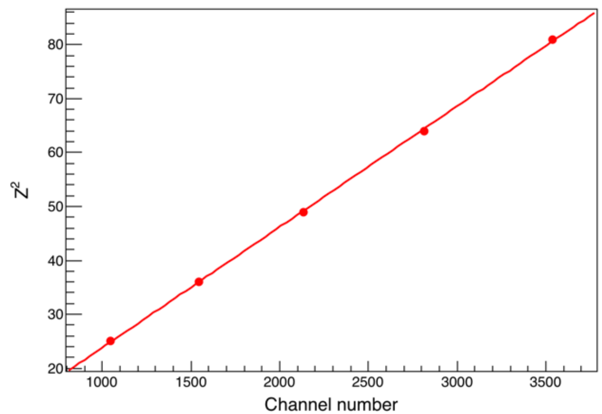

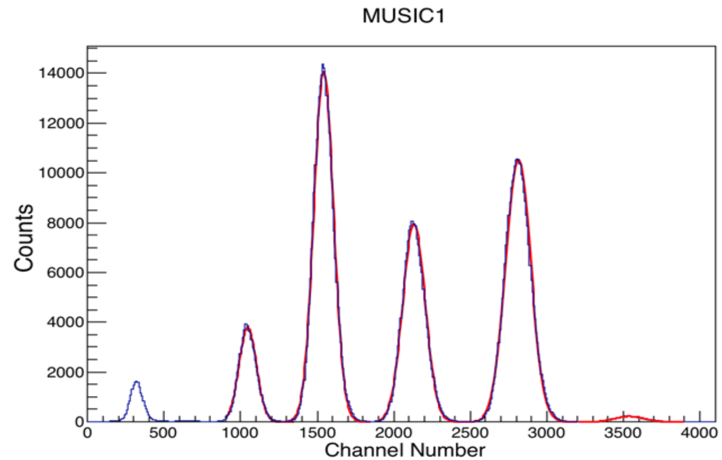

Points correspond to mean of the peaks obtained from gaussian fit of each peak in MUSIC energy spectrum

$$Z^2 = g*c + o$$

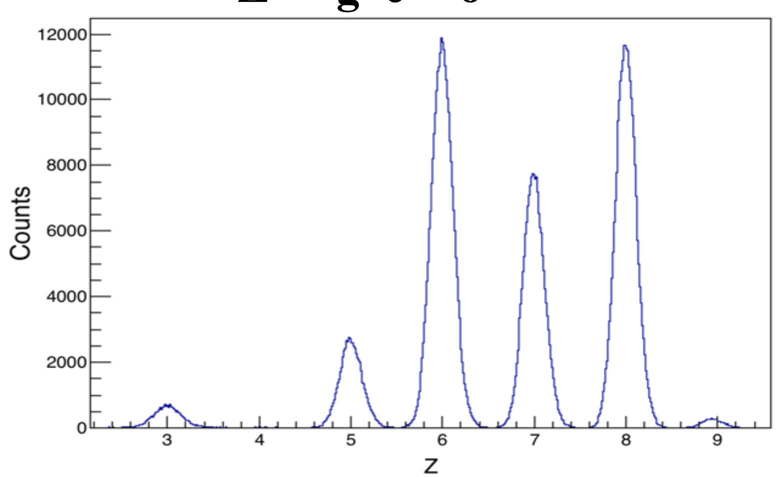

Calibrated MUSIC spectrum

Time Projection Chamber

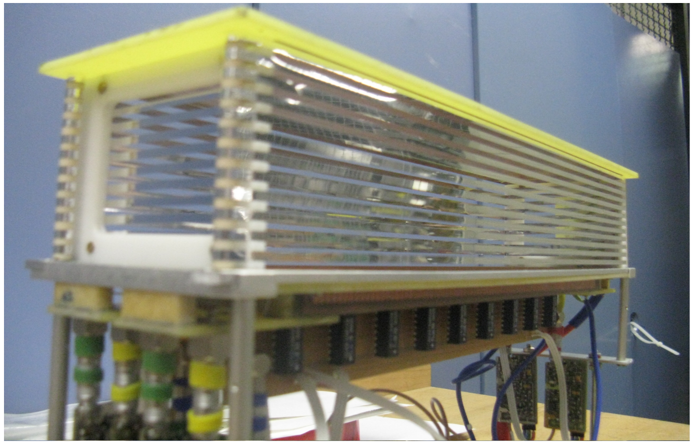

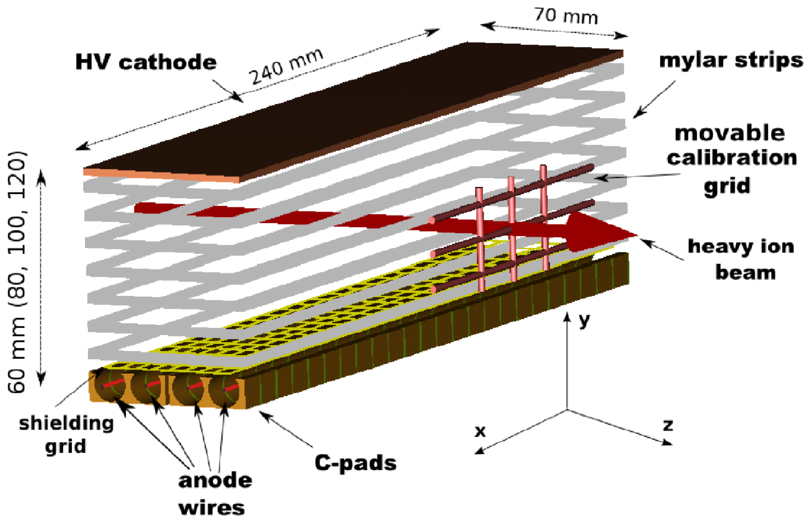

$$y = w_d t_a + y_{off}$$

$$x = w(t_l - t_r) + x_{off}$$

TPC Detector Calibration

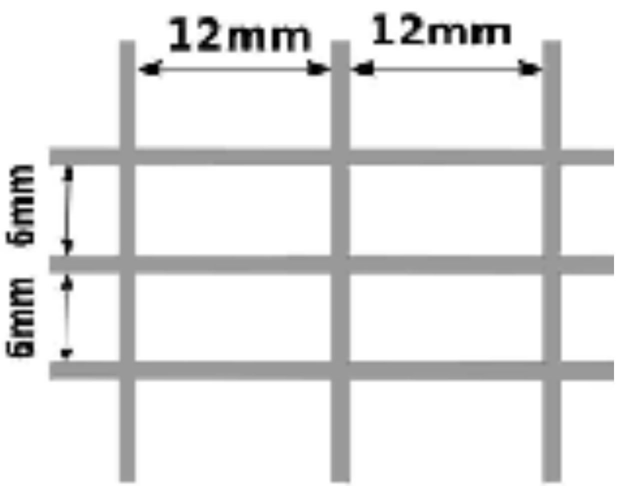

Schematic of scintillator fibres used for calibration of TPC

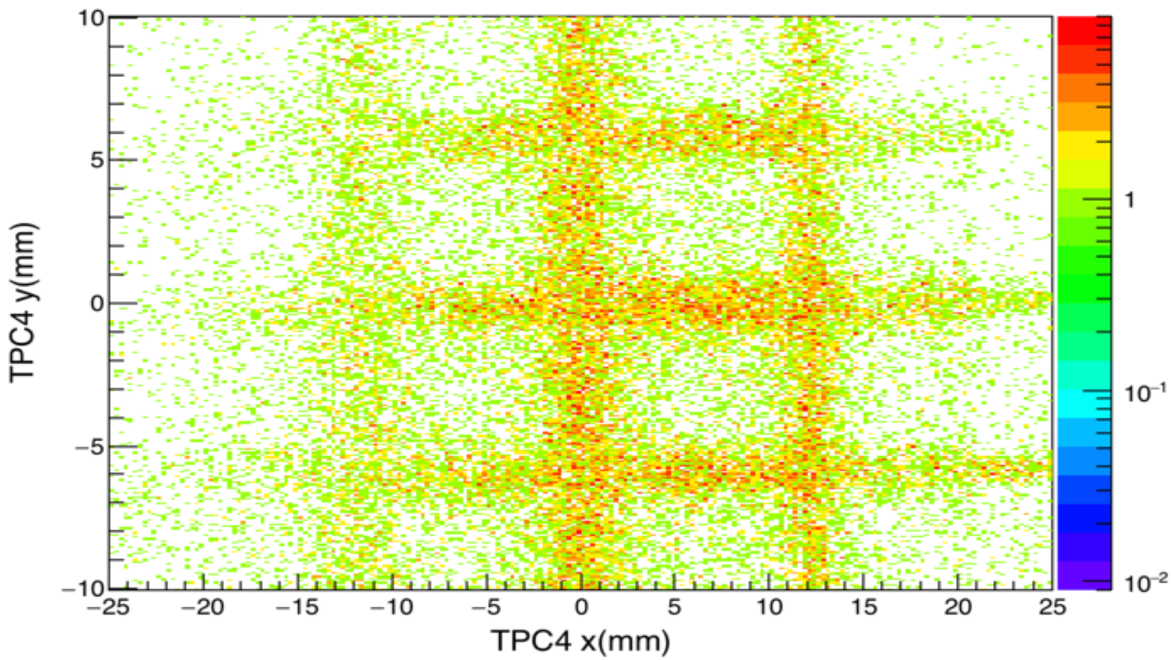

2 dimensional position spectrum showing structure of grid using stable beam.

Plastic scintillator

Scintillator:Energy deposited → light.
PMT: Light → electrical pulse

Each scintillator (at F2 and F4) had photomultiplier modules on both sides which gives two measurements for each detector.

$$TOF_{RR} = |T_{41R} - T_{21R}|$$

$$TOF_{LL} = |T_{41L} - T_{21L}|$$

$$TOF = \frac{(TOF_{RR} + TOF_{LL})}{2}$$

Calibration of TOF from Scintillator Detector

Time of flight is calibrated using stable primary beam with three different velocities.

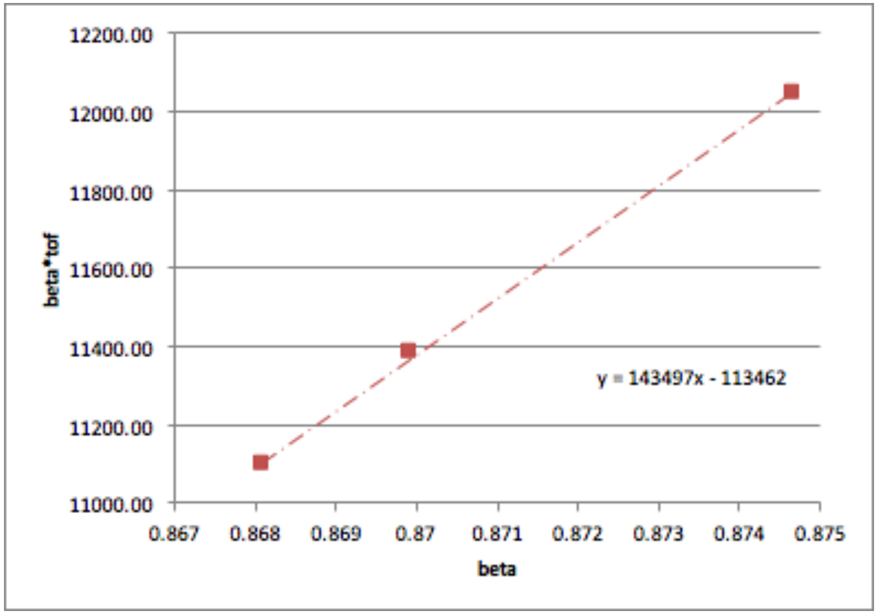

beta *tof =Flight path +beta*tof offset

tof offset = 143497

flight path =113462

$$\text{beta} = \frac{\text{flight path}}{\text{TOF} - \text{TOFoffset}}$$

Chiral effective field theory

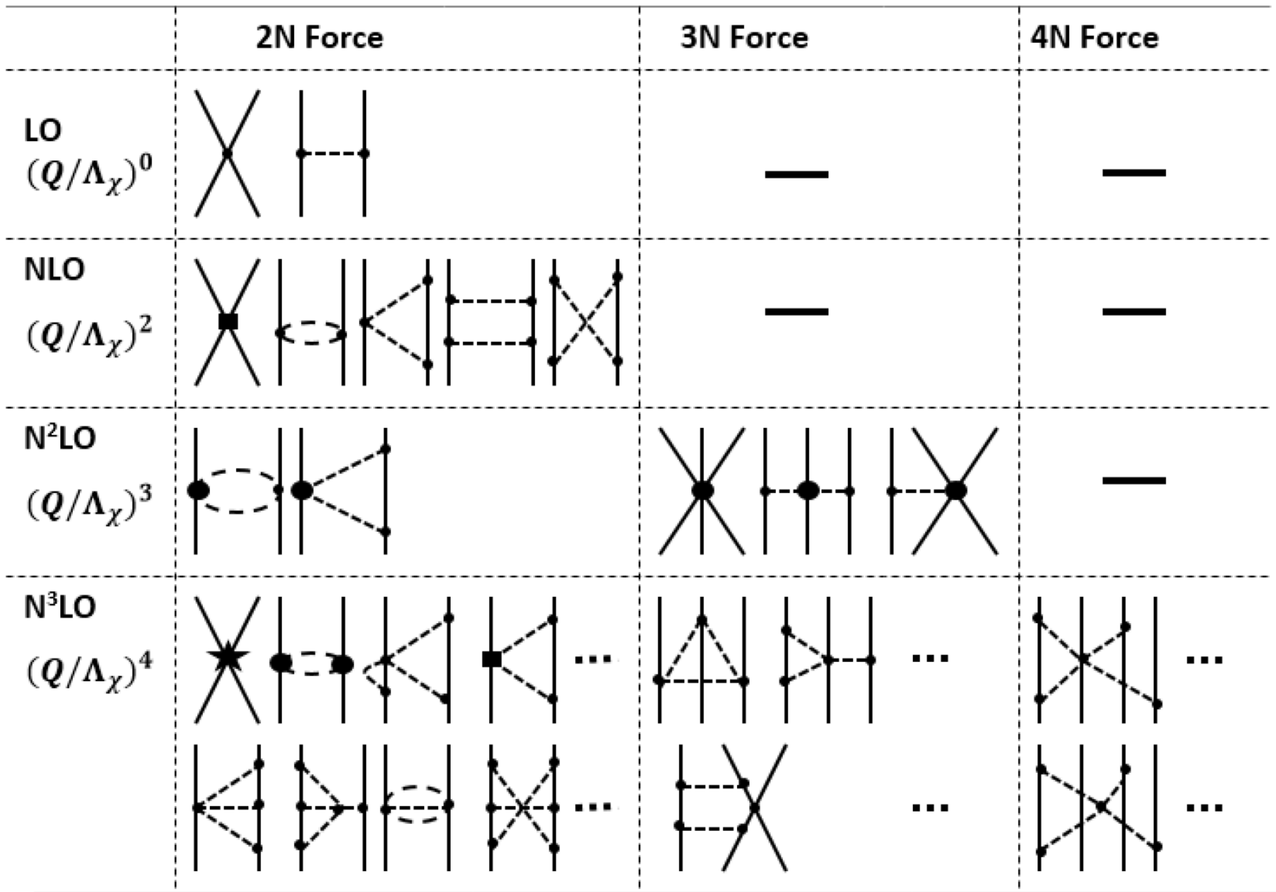

Fragment Separator GSI

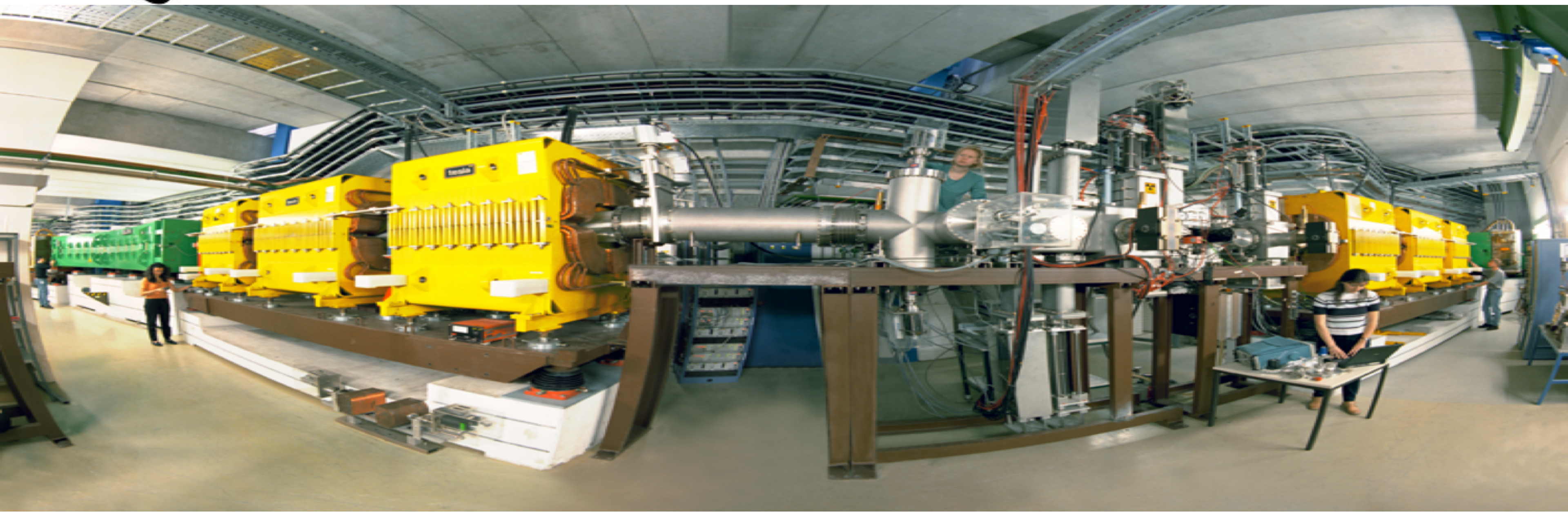

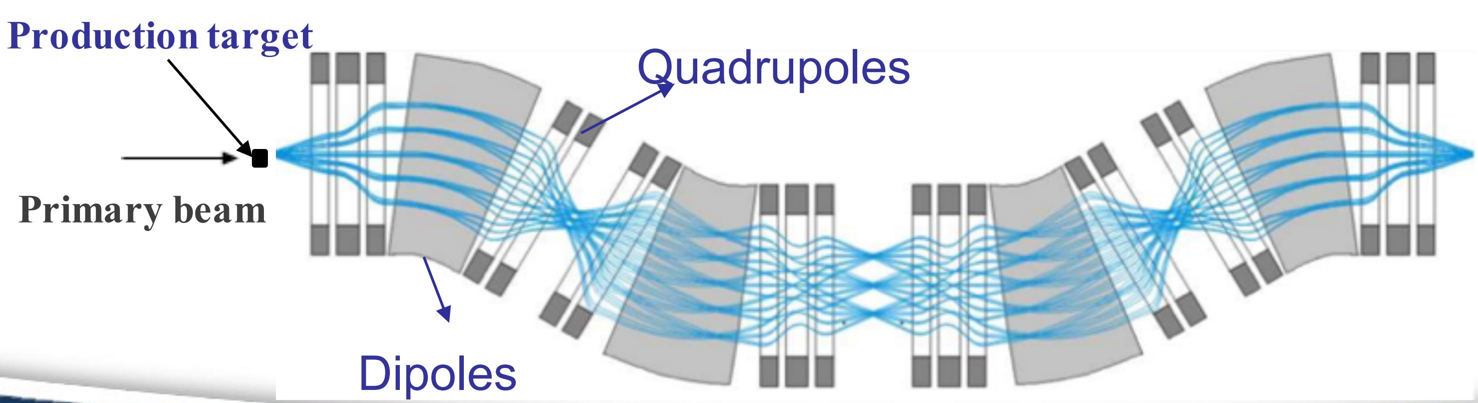

Charge Radii Relation to Point Proton Radii

Root mean square charge radius r_c is given by

$$\langle rc^2 \rangle = \langle rp^2 \rangle + \langle Rp^2 \rangle + \frac{N}{Z} \langle Rn^2 \rangle + \frac{3\hbar^2}{4mp^2c^2}$$

r_p is the radius of point proton distribution of a nucleus
R_p and R_n are the charge radii of free proton and free neutron
last term is so called Darwin–Foldy term

Matter Radii Related to Point Proton Radii and point neutron radii

$$\langle rm^2 \rangle = \frac{Z}{A} \langle {r_p}^2 \rangle + \frac{N}{A} \langle rn^2 \rangle$$

I. Tanihata et al. / Progress in Particle and Nuclear Physics 68 (2013) 215–313

Ion optics of Fragment separator

FRS working as an achromatic system with a dispersive mid-plane

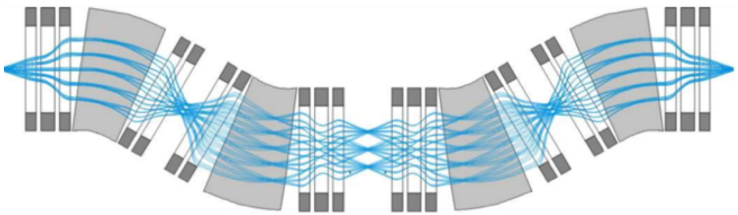

$$\begin{pmatrix} x \\ a \\ y \\ b \\ s \\ \delta_p \end{pmatrix} = \mathsf{M} \begin{pmatrix} x_0 \\ a_0 \\ y_0 \\ b_0 \\ s_0 \\ \delta_{p0} \end{pmatrix}.$$

$$a = \frac{dx}{ds} \qquad b = \frac{dy}{ds}$$

$$\delta_p = \frac{p - p_0}{p_0}$$

Magnification ← (x|x) … (x|δ) → D

$$\mathsf{M} = \begin{pmatrix} (x|x) & (x|a) & 0 & 0 & 0 & (x|\delta) \\ (a|x) & (a|a) & 0 & 0 & 0 & (a|\delta) \\ 0 & 0 & (y|y) & (y|b) & 0 & 0 \\ 0 & 0 & (b|y) & (b|b) & 0 & 0 \\ (s|x) & (s|a) & 0 & 0 & 1 & (s|\delta) \\ 0 & 0 & 0 & 0 & 0 & 1 \end{pmatrix}.$$

$$\delta_{\mathrm{F2}} = \frac{1}{D_{\mathsf{B}}} \left[x_{\mathrm{F4}} - (x|x)_{\mathsf{B}} x_{\mathrm{F2}} \right]$$

$$\delta_{\mathrm{F2}} = \frac{p - p_{\mathsf{B}}}{p_{\mathsf{B}}} = \frac{\chi - \chi_{\mathsf{B}}}{\chi_{\mathsf{B}}} \longrightarrow \chi = (1 + \delta_{\mathrm{F2}})\chi_{\mathsf{B}}$$

Focal plane location using position from TPC

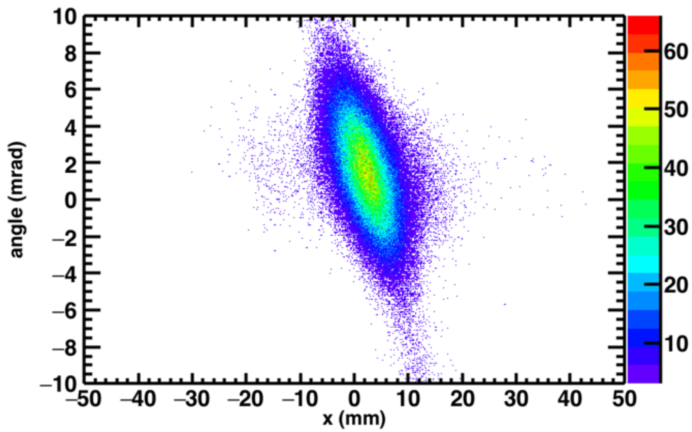

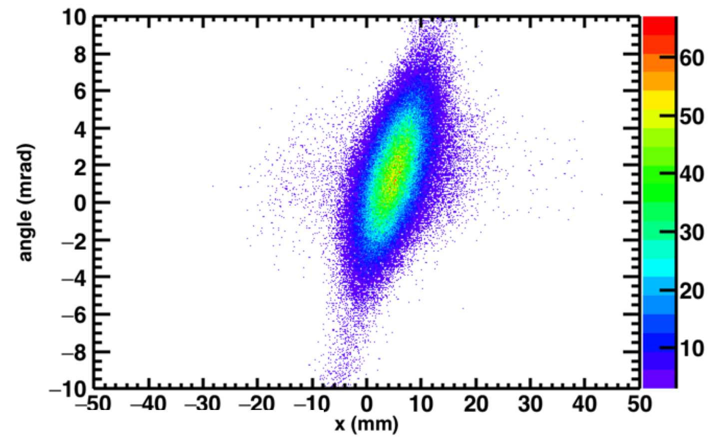

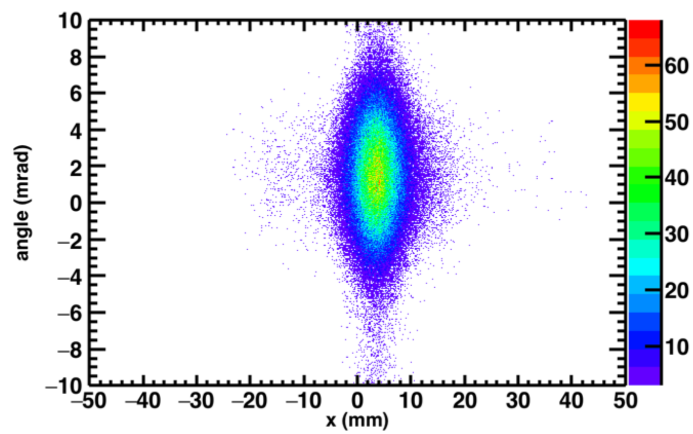

The x-position at the image plane is independent from the incident angle of the beam.

Nuclear Density distributions

Fermi or woods saxon form

$$\rho(r) = \rho_0/(1 + \exp((r - c)/z))$$

c is the radius of distribution to a point where density falls to half and z is diffuseness related to thickness of surface region.

Harmonic oscillator density

$$\rho(r) = \rho_0(1 + \alpha(r/a)^2)\exp(-(r/a)^2)$$

$$\alpha = \alpha_0 a_0^2/(a^2 + \tfrac{3}{2}\,\alpha_0(a^2 - a_0^2))$$

$$a_0^2 = (a^2 - a_p^2)A/(A-1)$$

$$\alpha_0 = (Z-2)/3; \quad a_p^2 = \tfrac{2}{3}\langle r^2 \rangle_{\text{proton}}$$

where a is the size parameter.

H. de Vries, C. W. de Jager and C. de Vries Atom. Data Nucl. Data Tables, 36 :495, 1987.

Proton Radii from σ_{cc}

Glauber Model

(R. J. Glauber:, 1959)

$$\sigma_R = \iint [1 - T(\mathbf{b})]\, db$$

At high energies

- Nucleons follow straight lines trajectories .
- Interaction of projectile and the target governed by individual nucleon nucleon cross section.

Probability of interaction [p(b)] $\propto \sigma_{nn}$, $\rho_P(r,z)$ and $\rho_T(r,z)dz$

Proton radii measured from σcc

Glauber Model applied successfully to B and C isotopes

Boron isotopes

(A. Estradé et al., Phys. Rev. Let.113, 132501,(2014)

- A thick neutron skin of 0.51± 0.11 fm was observed in ^{17}B.

($\delta R = 0.15 \pm 0.04$ fm for ^{208}Pb)

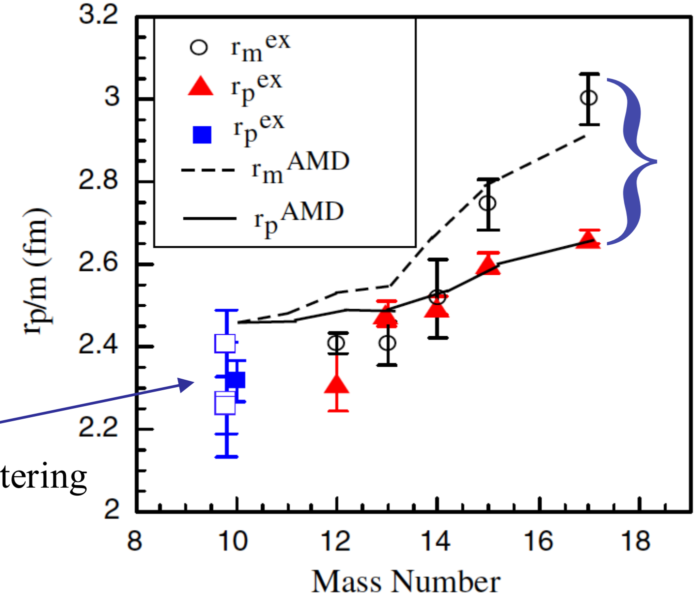

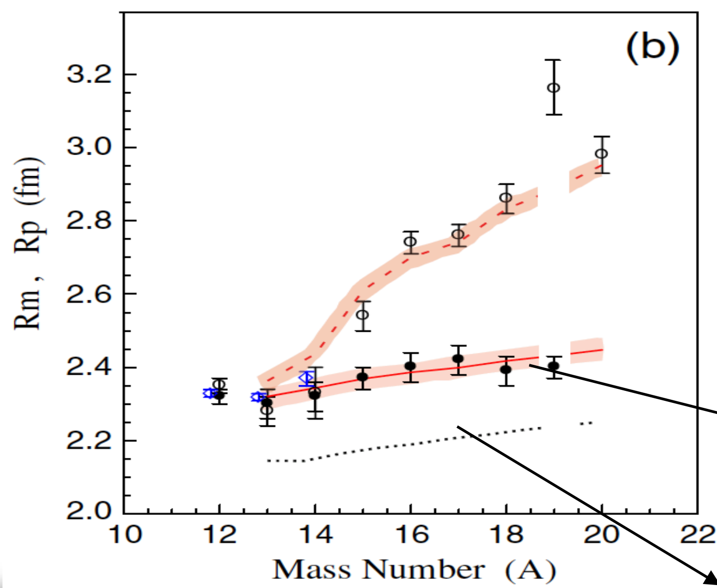

Carbon isotopes

R. Kanungo et al. Phys. Rev. Lett. 117, 102501 (2016).

Proton radii consistent with 3N forces

Proton radii with NN forces

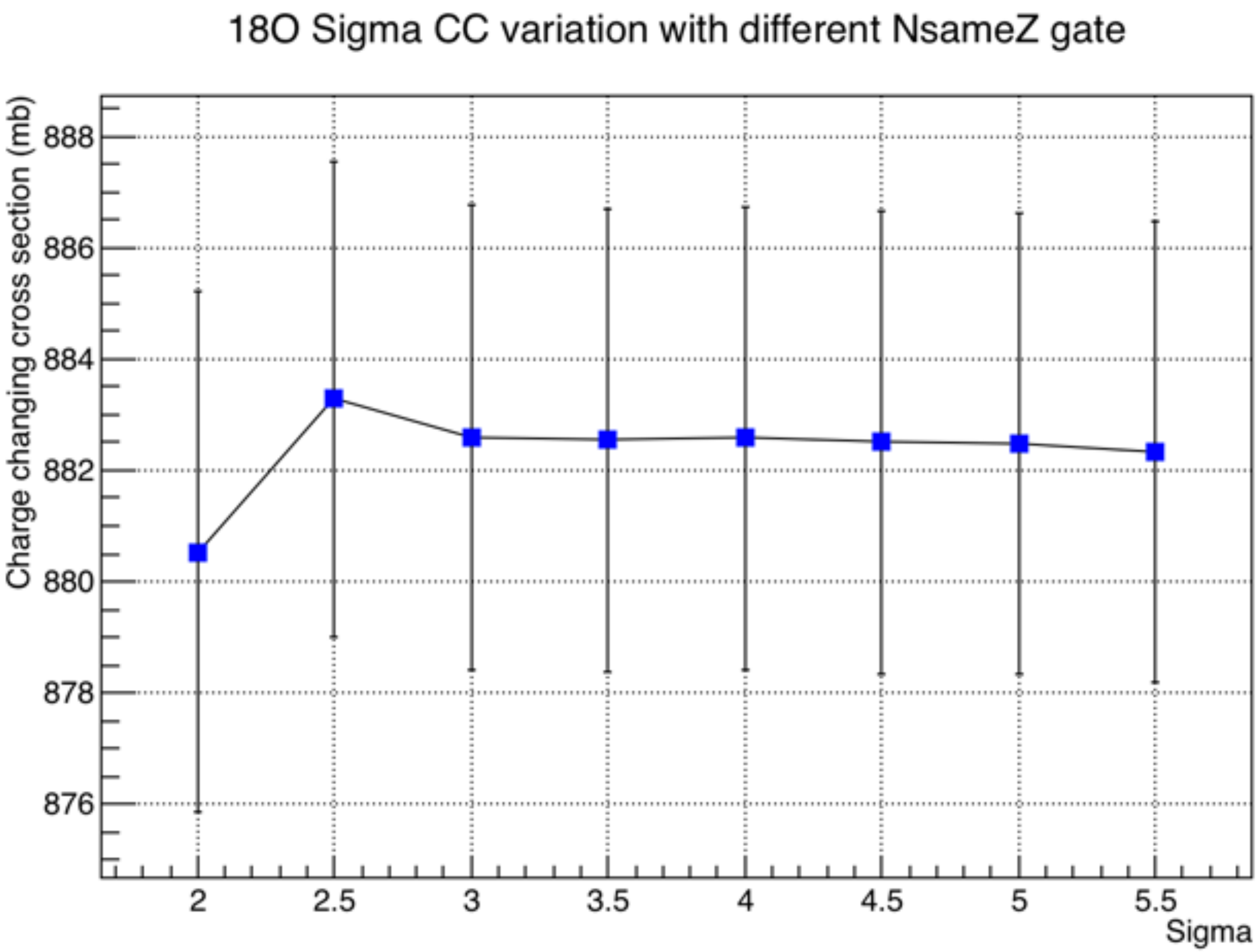
18O Sigma CC variation with different NsameZ gate
Charge changing cross section (mb)
888
886
884
882
880
878
876
2
2.5
3
3.5
4
4.5
5
5.5
Sigma

Nuclear Structure from Nuclear Radii

For Stable Nucleus

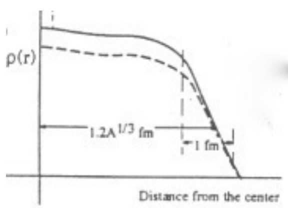

^{11}B (R ≈ 2 fm)

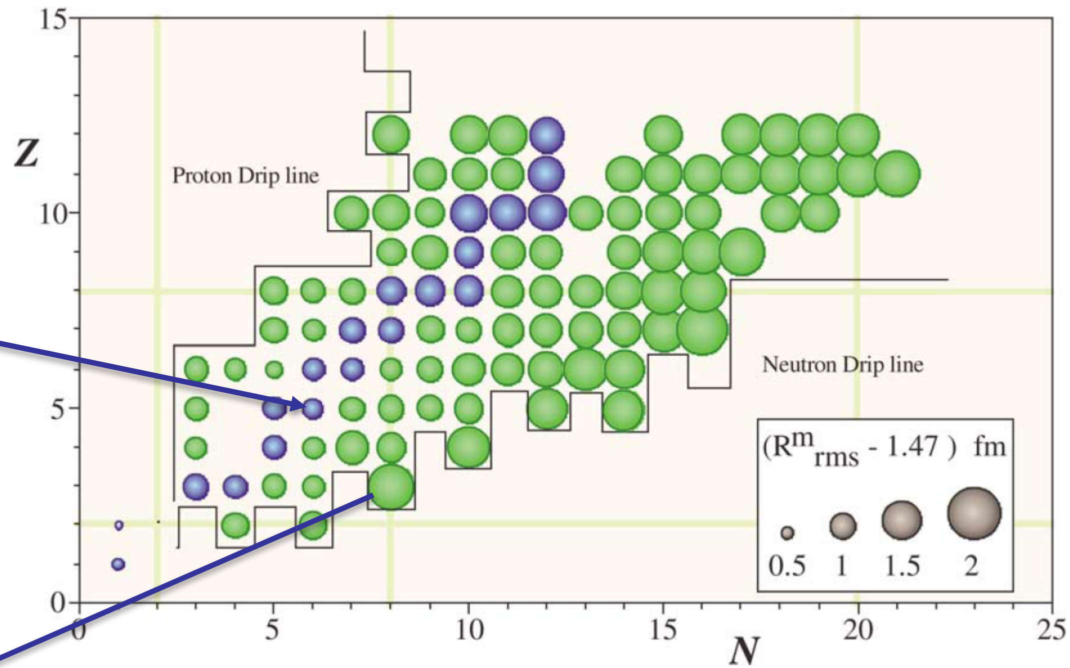

Neutron halo

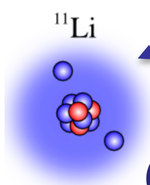

I. Tanihata, R. Kanungo / C. R. Physique 4 (2003) 437–449

(R ≈ 3.5 fm)

$R \neq 1.2\,A^{1/3}$

PID for 24O

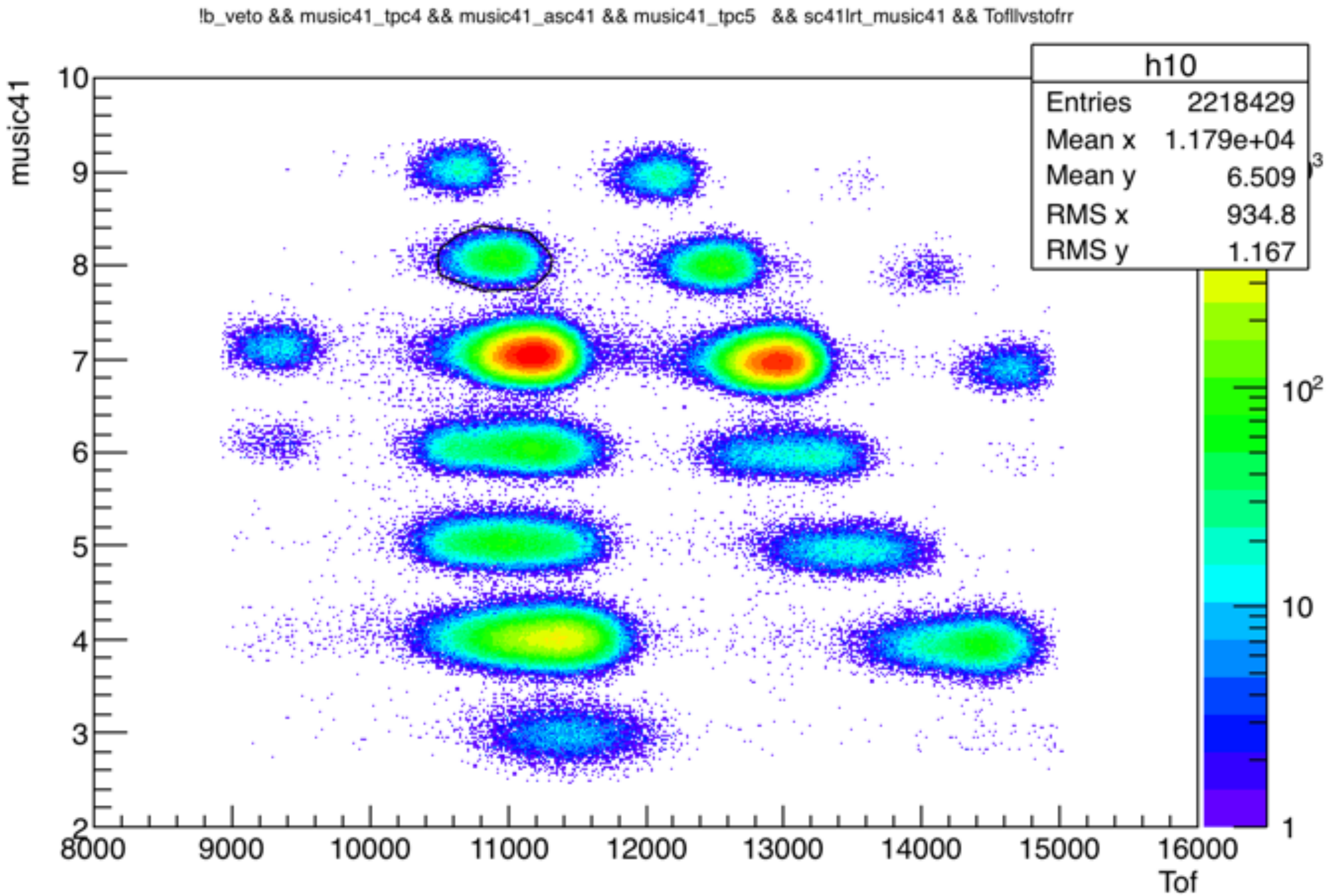

!b_veto && music41_tpc4 && music41_asc41 && music41_tpc5 && sc41lrt_music41 && Tofllvstofrr
h10
Entries 2218429
Mean x 1.179e+04
Mean y 6.509
RMS x 934.8
RMS y 1.167
music41
10
9
8
7
6
5
4
3
2
8000
9000
10000
11000
12000
13000
14000
15000
16000
Tof
10^2
10
1